**PREPARED FOR THE U.S. DEPARTMENT OF ENERGY,
UNDER CONTRACT DE-AC02-76CH03073**

PPPL-3529
UC-70

PPPL-3529

Negative Ion Density Fronts

by

Igor Kaganovich

December 2000

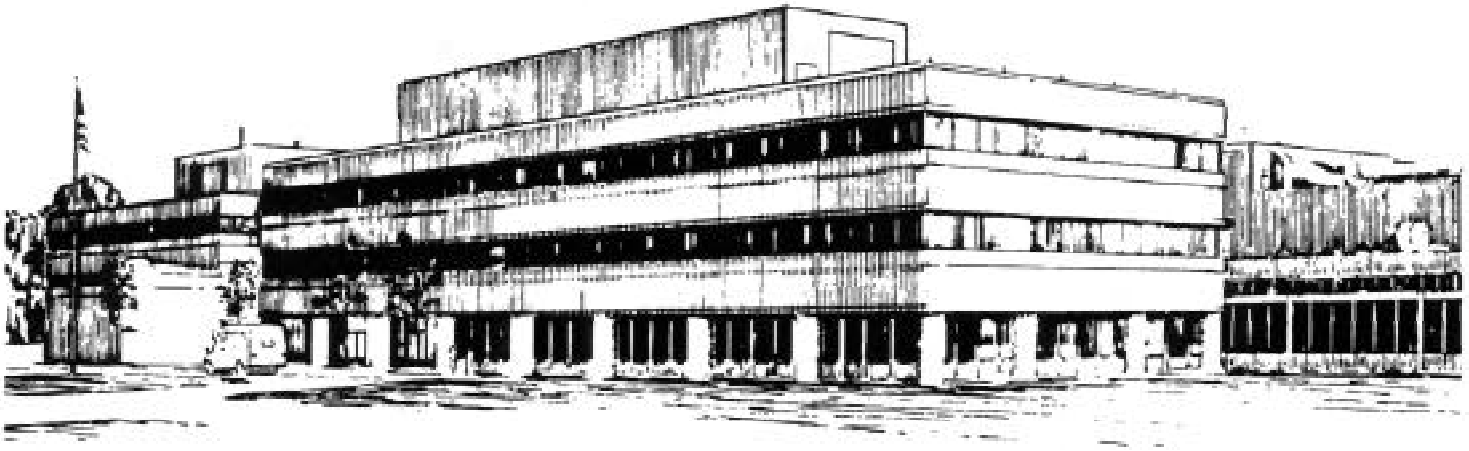

**PRINCETON PLASMA PHYSICS LABORATORY
PRINCETON UNIVERSITY, PRINCETON, NEW JERSEY**

PPPL Reports Disclaimer

Availability

This report is posted on the U.S. Department of Energy's Princeton Plasma Physics Laboratory Publications and Reports web site in Calendar Year 2000. The home page for PPPL Reports and Publications is: http://www.pppl.gov/pub_report/

DOE and DOE Contractors can obtain copies of this report from:

U.S. Department of Energy
Office of Scientific and Technical Information
DOE Technical Information Services (DTIS)
P.O. Box 62
Oak Ridge, TN 37831

Telephone: (865) 576-8401

Fax: (865) 576-5728

Email: reports@adonis.osti.gov

This report is available to the general public from:

National Technical Information Service
U.S. Department of Commerce
5285 Port Royal Road
Springfield, VA 22161

Telephone: 1-800-553-6847 or
(703) 605-6000

Fax: (703) 321-8547

Internet: http://www.ntis.gov/ordering.htm

Negative ion density fronts

Igor Kaganovich[1]

Plasma Physics Laboratory, Princeton University, NJ 08543

Negative ions tend to stratify in electronegative plasmas with hot electrons (electron temperature T_e much larger than ion temperature T_i, $T_e >> T_i$). The boundary separating a plasma containing negative ions, and a plasma, without negative ions, is usually thin, so that the negative ion density falls rapidly to zero – forming a negative ion density front. We review theoretical, experimental and numerical results giving the spatio-temporal evolution of negative ion density fronts during plasma ignition, the steady state, and extinction (afterglow). During plasma ignition, negative ion fronts are the result of the break of smooth plasma density profiles during nonlinear convection. In a steady-state plasma, the fronts are boundary layers with steepening of ion density profiles due to nonlinear convection also. But during plasma extinction, the ion fronts are of a completely different nature. Negative ions diffuse freely in the plasma core (no convection), whereas the negative ion front propagates towards the chamber walls with a nearly constant velocity. The concept of fronts turns out to be very effective in analysis of plasma density profile evolution in strongly non-isothermal plasmas.

PACS numbers: 52.35 Lv, 52.35Tc, 52.75 Rx

[1] e-mail: ikaganov@pppl.gov,

I. Introduction

Negative ions are readily formed in plasmas containing halogen gases and elements of oxygen group of periodic table. Historically, processes in electronegative (EN) plasmas have attracted considerable attention in the connection with problems of atmospheric electricity. Interest in EN plasmas has been expanded recently due to wide-spread applications in materials processing. As a rule, the plasmas, used in these processes, are strongly electronegative –i.e. the negative ion density is large compared to the electron density. Some specific application areas include semiconductor manufacturing [1], use of negative ions to eliminate notching [2], negative ion sources [3], and the ionospheric D-layer [4]. The theory of plasma transport in electronegative gases can be transferred to processes in the dusty plasmas [5], which play important roles in modern ecology and plasma technology. Dust particles in plasmas are typically negatively charged, and can be considered as large negative ions.

The plasmas used in technological applications are created by continuous wave (CW) or pulsed discharges. Pulsed EN plasmas (in which the power is turned on and off with a predetermined period and duty cycle) have been shown to offer important advantages compared to their CW counterparts. Properties of deposited films can be altered [6], and etch and deposition rate can be maintained despite the lower average power [7]. Recently, it has been recognized that pulsed plasmas may also ameliorate anomalous etch profiles (e.g. notching) and other forms of charge damage that occur in conventional continuous wave discharges [2]. The ratio of chemical species present in the plasma can be varied, e.g., production of negative ions can be increased in pulsed negative ion sources compared to conventional CW discharges [3].

Negative ions are difficult to extract from CW plasmas, because the ambipolar electrostatic field arises to counteract electron diffusion in plasmas, and as a result negative ions are trapped in this field. When power is turned off in the afterglow, electrons disappear rapidly because of diffusion to the walls and attachment to gas molecules. Late in the afterglow, the electron density and temperature are too low for any significant electrostatic fields to exist, and a transition occurs from an electron-dominated plasma to a positive ion - negative ion (ion-ion) plasma [8, 9, 10]. After that time, it is possible to extract negative ions from the plasma. Numerous applications call for a fundamental study of nonstationary EN plasmas.

We focus on collisional plasma transport where the ion mean free path is smaller than the plasma chamber dimensions. The study of collisional plasmas with negative ions has a long history. Nevertheless, the theoretical understanding of their behavior lags behind the progress in applications of electronegative gases and the needs of technology. The reason for this consists in complex self-consistent character of the multi-species plasma transport. The generation, mutual conversion and removal of the charged particles are determined by complicated sequences of plasma-chemical reactions, which are not well understood in many cases. The fluxes of ions and electrons are controlled by diffusion and drift in the self- consistent electric fields. It is widely known, that even neutral gases with a combination of chemical kinetics and diffusion results in development of surprising and complicated synergetic phenomena of self-organization [11]. In plasmas the transport of charged particles is controlled not only by diffusion, but also by the self-consistent electric fields. It follows that the form of the spatial profiles of charged particles densities becomes far more diverse. Even a simple classification of possible regimes turns out to be non-trivial.

The transport equations for a quasineutral plasma are not too complicated and allow comparatively simple numerical solutions. On the other hand, many input parameters determine the

plasma profiles; and as a result any single calculation for a given set of the plasma chemical rates is not too instructive and predictive for other input parameters. In order to formulate scaling laws, and to obtain the criteria for transitions between different transport scenarios, it is necessary to perform a considerable volume of numerical calculations. It is therefore not too easy to extract an understanding of underlying physics out of computer results. In this paper the physical insight on transport of negative ions developed during last decade will be presented.

The first approaches to investigate charged particle transport in electronegative plasmas consisted in attempts to generalize the widely known concept of ambipolar diffusion [12, 13]. In the first of these [12] the electric field was eliminated from the equations for the plasma transport by postulating a Boltzmann equilibrium for the negative ions. In the second approach [13] the ad hoc assumption of similar density profiles for all charged species was made. It will be shown below that in contrast to the electrons, a Boltzmann equilibrium for the negative ions occurs only at rather low pressures. The other assumption of similarity of all charged species profiles is correct only if $T_e=T_i$ and boundary condition of zero densities is used. In all other cases, even if the initial profiles are similar, in the process of evolution this similarity will be destroyed. Moreover, if the electron temperature T_e is much larger than the ion temperature T_i, the effective diffusion coefficient for negative ions, derived in the assumption of similar profile, is negative. This fact contradicts to conventional meaning of diffusion. It means, in our opinion, that such a description is misleading, and it is necessary to seek solution in some other way. A similar conclusion has been reached by R. Franklin, et. al. in Ref. 14.

In the general case the field-driven fluxes of the charged particles are of a complex nature, and the electric field must be explicitly retained in the transport equations. It was shown in [15, 16] that the linear equation for ambipolar diffusion is strictly valid only in the case of so called simple

weakly ionized plasma, which consists of electrons and one species of the positive ions with constant field-independent mobilities and diffusion coefficients. Indeed, in the case of two-component plasma (positive ions and electrons with densities $p=n_e$), and assuming Boltzmann equilibrium for electrons, $E = -T_e/e\nabla(\ln n_e)$, the drift flux of positive ions is reduced to an effective linear (ambipolar) diffusion flux, $\mu_i eE\, p = -\mu_i T_e \frac{p}{n_e}\nabla n_e = -\mu_i T_e \nabla n_e$. Here, μ_i is ion mobility. If plasma consists of two or more sorts of ions, the flux of any given species of the charged particles depends not only on its own density gradient, but also on the density gradients of all the other species. For example, the presence of negative ions substantially influences the charged species fluxes in EN plasmas. In a plasma containing negative ions (with density n), the drift flux of positive ions is a nonlinear function of densities, $\mu_i eE\, p = -\mu_i T_e \frac{p}{n_e}\nabla n_e$ ($p=n+n_e$), and described by convection, with a velocity $u_p = \mu_i eE = -\mu_i T_e \frac{\nabla n_e}{n_e}$ that depends nonlinearly on electron densities, and via quasineutrality condition ($n_e = p-n$) depends nonlinearly on the negative ion density too. Under some plasma conditions the negative ions can also be in Boltzmann equilibrium with the electric field ($-\mu_i neE - -\mu_i T_i \nabla n \approx 0$). In this case the negative ion density is an explicit function of electric field and the positive ion flux is proportional to the positive ion density gradient, with the factor, which is a nonlinear function of the positive ion density [12].

In any case, because of the nonlinearity of the equations, and the transitions between regions where different assumptions are valid it is necessary to start from a qualitative understanding of the basic equations to develop a methodology for solving the transport equations under various conditions. It turns out that, for this aim, separation of the plasma volume into different regions is an

effective approach. In each of these regions different physical processes dominate. The proposed methodology is based on *a fundamental phenomenon, which appears in multi-component plasma that the plasma stratifies into regions with different ion composition [17-21]*. For example electronegative plasmas with hot electrons often separate into core region, containing the negative ions (electronegative region), and an electron-ion edge region, near the walls, which contains essentially no negative ions (electropositive region). The electrostatic field is very low in the core and relatively high in the edge region. At the transition between the two regions the strong edge electric field pushes negative ions inwards, so that the negative ion density falls precipitously towards the edge, and a negative ion front forms.

In a description of boundaries between the electronegative and electropositive regions the concept of shock-like transitions is very effective. These regions of steep variation of the species densities, which separate regions of smooth profiles, are analogous to shocks, which are widely known in hydrodynamics [22]. At low pressures, double layer may form separating the ion-ion core and the electron-ion edge regions. A double layer is a collisionless structure, in which the ion mean free path λ_i is larger than a width of shock δ, such that ion inertia is important. Formation of the fronts has been attributed to nonlinear ion acoustic waves [23] for collisionless plasmas. Double layers have been shown to occur in steady-state collisionless, $\lambda_i > L$, (L is a half of the interelectrode distance) [24] or collisional [25] plasmas, $\delta < \lambda_i < L$. Shocks can be also formed in collisional plasma, $\lambda_i < \delta < L$. As early, as a century ago, the idea that shock-like structures form in multi-species current-carrying media was formulated for electrolytes [26, 27]. The idea was applied to gas discharges [15, 16, 28] and semiconductor plasmas [17, 29]. In papers [20, 21] it was shown, that similar narrow shock-like structures- fronts, which separate the plasma regions with smooth

profiles and different ion composition, naturally arise also in currentless collisional non-isothermal plasma.

These negative ion density fronts have been observed experimentally in steady state oxygen rf glow discharges sustained in capacitively-coupled parallel plate reactors [30, 31]. The measured negative ion density profile tends to form a front at the electrode. Examples of fronts are shown in Figs.1-4 for stationary rf discharges.

Negative ion fronts also exist during ignition and extinction (afterglow) of electronegative plasmas, and are shown in Fig. 5 and 6, respectively. The spatio-temporal evolution of such fronts has been studied theoretically and by a numerical "experiment" in an argon/oxygen pulsed discharge [21, 32]. In pulsed discharges, power to the discharge is modulated (e.g., square wave modulation) with a specific frequency and duty ratio. During plasma ignition (power on), self-sharpening negative ion density fronts develop and move towards the plasma center, in analogy with gasdynamic shocks, see Fig.5.

During the afterglow, negative ion fronts exist when $T_e >> T_i$, and move towards the chamber walls. However, the latter fronts are of a completely different nature and have no direct analogy with gasdynamic shocks. The propagation of gasdynamic shocks is dominated by convection, and dissipative mechanisms (viscosity, thermal conductivity, etc.) influence only the internal shock structure. In contrast, during the afterglow negative ions diffuse nearly freely in the ion-ion core (the role of drift is negligible), slow down as they approach the edge region due to increasing electrostatic field. The drift flux due to the field is directed towards the plasma center and, at the periphery, nearly compensates the diffusion flux, which is in the opposite direction. The resulting negative ion velocity is directed outwards. It turns out that, although the main evolution is by diffusion, the negative ion front propagation speed is nearly constant for constant electron and

ion temperatures, as opposite to the $\sqrt{D_i t}$ dependence for diffusive front propagation. The negative ion front is a new type of nonlinear structure, different from gasdynamic nonlinear waves, and beyond the classification of dissipative structures made in Ref. 11.

II **Description of the model**

It is assumed that the ion mean free path is smaller than the characteristic chamber dimension and we examine one-dimensional transport of species in parallel plate geometry. For a collisional plasma, the species fluxes are described by a drift-diffusion model, $\Gamma_k = -D_k \partial n_k / \partial x - \mu_k n_k e E$, where D_k and μ_k are the *k*-species diffusion coefficient and mobility, respectively, related by the Einstein relation $D_k = T_k \mu_k$; T_k is the *k*-species temperature. Considering only one positive and one negative ion species, the self-consistent electrostatic field is found from the condition of zero net current $j = e(\Gamma_p - \Gamma_n - \Gamma_e) = 0$ and is given by

$$eE = \frac{-D_e \nabla n_e - D_n \nabla n + D_p \nabla p}{\mu_e n_e + \mu_p p + \mu_n n}. \qquad (1)$$

Subscripts *p*, *n*, and *e* correspond to positive ions, negative ions, and electrons, respectively, and $\nabla = \frac{\partial}{\partial x}$. Ion diffusion coefficients are factor 10^{-5} smaller than the electron diffusion coefficient, and ion diffusion fluxes may be neglected in Eq.(1). If the electron density is such that $\mu_e n_e >> \mu_n n, \mu_p p$ and its gradient is not too small, electrons are described by a Boltzmann equilibrium:

$$E = -T_e / e \nabla (\ln n_e), \qquad (1a)$$

which gives an explicit relation between electric field and the logarithmic electron density gradient. Below we shall only consider case $n_e\mu_e >> (\mu_p p + \mu_n n)$, where the electric field is explicitly related by the Boltzmann relation for electrons. Note, that electronegativity n/n_e can be large for this case, since ratio μ_e / μ_p is typically of the order of few hundreds. The transition to ion-ion plasma $n_e\mu_e << (\mu_p p + \mu_n n)$ is described at length in Ref. 32.

Eq. (1) for the electric field, along with the continuity equations for negative ion (Eqs.2a) and positive ion number density (Eqs.2b), and the electroneutrality constraint (Eqs.2c), and an equation for the electron temperature (see below) yield a complete system of equations that describes the spatio-temporal evolution of charged species densities, fluxes, and electric field

$$\frac{\partial n}{\partial t} - \mu_n \frac{\partial}{\partial x}\left(T_i \frac{\partial n}{\partial x} - eEn \right) = \nu_{att} n_e - \gamma_d n - \beta_{ii} np \,, \tag{2a}$$

$$\frac{\partial p}{\partial t} - \mu_p \frac{\partial}{\partial x}\left(T_i \frac{\partial p}{\partial x} + eEp \right) = Z_{ioniz} n_e - \beta_{ii} np \,, \tag{2b}$$

$$n_e = p - n \,. \tag{2c}$$

In the above equations, β_{ii} is the ion-ion recombination rate coefficient, and Z_{ioniz}, ν_{att}, and γ_d, are the ionization, attachment, and detachment frequencies, respectively. Zero densities at the wall or Bohm criterion maybe used for boundary conditions [33].

In the fluid approximation, the continuity Eqs. (2) are supplemented by an equation for the electron temperature [1]:

$$\frac{\partial}{\partial t}\left(\frac{3}{2} n_e T_e \right) + \frac{\partial q_e}{\partial x} = W - \sum_i R_i H_i \,, \tag{3}$$

where $q_e = -\chi_e \partial T_e / \partial x + 2.5 T_e \Gamma_e$ is the electron energy flux, W is the power density deposited in the electron gas, and R_i is the rate of electron impact process *i* having activation energy H_i.

Boundary conditions on Eq. (3) are zero flux at the discharge center and $q_e = 2.5 T_e \Gamma_e$ at the plasma-sheath boundary. A kinetic description replacing the fluid approach in (3) is preferred if, the electron distribution function departs significantly from Maxwellian, see for example Refs. 31, 34, 35.

In solving these equations analytically it is necessary to make further assumptions. We consider the species transport properties (diffusion coefficients, mobilities, and the attachment, detachment and recombination rate coefficients) as field- and composition independent constants. In reality the electron attachment, detachment, and especially ionization rates depend on the electron energy distribution function, which has to be found simultaneously [34, 35]. The ionization frequency represents an eigenvalue of the electron density balance for a steady-state discharge. For plasma bulk calculation it is often not necessary to include sheath properties, unless the characteristics of the energy input are considered [1, chap11] and we shall not consider the sheath here.

The system of Eqs. (1, 2) is a complicated system of nonlinear equations. Indeed, substituting the expression for electric field, Eq. (1a), into the continuity equations for electrons and negative ions and using the electroneutrality constraint yields a new system of equations:

$$\frac{\partial n}{\partial t} - \frac{\partial}{\partial x}\left(\mu_n T_i \frac{\partial n}{\partial x} - un \right) = \nu_{att} n_e - \gamma_d n - \beta_{ii} np \,, \tag{4a}$$

$$\frac{\partial n_e}{\partial t} - \frac{\partial}{\partial x}\left(D_{eff} \frac{\partial n_e}{\partial x} \right) - \frac{\partial}{\partial x}\left((\mu_p - \mu_n) T_i \frac{\partial n}{\partial x} \right) = (Z - \nu_{att}) n_e + \gamma_d n \,, \tag{4b}$$

$$n_e = p - n \,, \tag{4c}$$

where $u = \mu_n T_e \frac{\partial ln n_e}{\partial x}$, and $D_{eff} = \frac{T_e(\mu_p p + \mu_n n)}{n_e} + \mu_p T_i$ is a function of $\frac{n}{n_e}$. The system of Eqs.(4) may be more familiar than the initial system of Eqs. (2), since Eq.(4b) is a diffusion-type equation, in contrast to the diffusion-drift-type of Eqs.(2a,b).

III. Small signal propagation

We start the analysis of the system of Eqs. (4) by studying small signal propagation in unbounded plasma neglecting source and sink terms on the right hand side of Eqs.2, and neglecting ion diffusion terms compared with drift $\frac{T_i}{n}\frac{\partial n}{\partial x} << \frac{T_e}{n_e}\frac{\partial n_e}{\partial x}$. The ion and electron density variations δn_α are taken to be of the form $\delta n_\alpha \, exp(-i\omega t + ikx)$. If the inhomogeneity of the background plasma has to be taken into account, in particularly the electron density gradient: $\frac{\partial n_e}{n_e \partial x} \equiv \frac{1}{L_e} \neq 0$. The derivations are easier to perform in the limit of small-scale perturbations $|kL_e| >> 1$. Linearization of system (4) results in two modes,

$$\omega_1 = -iD_{eff}k^2. \qquad (5a)$$

$$\omega_2 = u_{eff}k\,,\ u_{eff} = \frac{\mu_n \mu_p}{\mu_n n + \mu_p p}\frac{T_e \partial n_e}{\partial x}. \qquad (5b)$$

The first mode (5a) corresponds to diffusion, see Eq. 4b. In the second mode the signal moves with a velocity $u_{eff} = \frac{\mu_p n_e}{\mu_n n + \mu_p p} u$ a factor $\frac{\mu_p n_e}{\mu_n n + \mu_p p}$ different from the negative ion drift velocity *u*. The theoretical predictions Eqs. (5b) were verified by numerical modeling. The propagation of a small perturbation is shown in Fig.7 for three different values of electronegativity

(n/n_e). When the electronegativity $n/n_e << 1$ is small, u_{eff} coincides with the drift velocity of negative ions $u_{eff} \approx u$. In the opposite case, when $n/n_e >> 1$, u_{eff} is much lower than the drift velocity *u,* and perturbations drift more slowly as can be seen in Fig.8. Theoretical calculations of the signal speed coincide exactly with results of numerical simulations [36].

IV. Nonlinear evolution of negative ion density profiles and formation of negative ion fronts.

In the previous section we found that the speed of negative ion density perturbation depends significantly on negative ion density. It means that different parts of profile of large perturbations of negative ion density move with different velocity, and nonlinear evolution results in profile modification. To analyze the nonlinear evolution of the negative ion density profile it is convenient to derive the small signal propagation velocity Eq. (5b) in another way. We shall use the fact that in the limit $|kL_e| >> 1$ $\omega_1 >> \omega_2$. Consequently, during evolution of narrow perturbations of negative ion density, the electron density perturbations are much smaller than ion density perturbations. Indeed, from Eq.4b it follows $\delta n \sim \omega_1/\omega_2 \delta n_e >> \delta n_e$. Accordingly, electron flux varies much more slowly than ion flux, and can be assumed nearly constant ($\frac{\partial n}{\partial t} = \frac{\partial}{\partial x}\Gamma_n$ $\frac{\partial n_e}{\partial t} = \frac{\partial}{\partial x}\Gamma_e$) $\delta n >> \delta n_e \Rightarrow \frac{\partial \Gamma_n}{\partial x} >> \frac{\partial \Gamma_e}{\partial x}$. Substituting $\frac{\partial n_e}{\partial x}$ from the expression for electron flux $\Gamma_e = -D_{eff}\frac{\partial n_e}{\partial x}$, and dropping all terms except convection term, Eq.(4a) can be rewritten in the form:

$$\frac{\partial n}{\partial t} + \frac{\partial}{\partial x}(\Gamma_n) = 0, \qquad (6a)$$

$$\Gamma_n = -\Gamma_e \frac{\mu_n n}{\mu_n n + \mu_p p} \qquad (6b)$$

A plot of the function $\Gamma_n / \Gamma_e(n/n_e)$ is shown in Fig.8. As discussed above, variation of perturbations of electron flux and electron density can be neglected compared with negative ion perturbation. So that Eq.(6a) simplifies to

$$\frac{\partial n}{\partial t} + u_{eff}(n)\frac{\partial}{\partial x} n = 0, \qquad (6c)$$

where the small signal propagation velocity $u_{eff} = \frac{\partial \Gamma_n}{\partial n}$ coincides with the previous estimate Eq.5b, but still remains valid for nonlinear perturbations too. The evolution of nonlinear negative ion density perturbation is shown in Fig.9. The solution of Eq. (6c) is $n = n_0(x - u_{eff}(n)t)$ [22], each point of the initial profile $n_0(x)$ moves with its own velocity $u_{eff}(n)$. Accordingly, consistent with theoretical predictions, in Fig.9 and 5 the regions of small negative ion density move faster than regions of large negative ion density. As a result, the front profile spreads out, the back profile steepens, breaks and forms anon density discontinuity (Fig.9 and 5). It is fully analogous to ordinary gasdynamics; two types of discontinuities are possible; one type is a shock, which is stable, and satisfy the evolutionality criterion (back front of the signal); and unstable ion density discontinuities, which structure is unstable and spreads proportionally to time (front of the signal in Fig.9). To prevent confusion with ordinary gasdynamic shocks, we shall call the ion density discontinuities *ion density fronts*. In some sense, these fronts are even more fundamental, than, the usual gasdynamic shocks, since they result from the first order equation (6c), while, in order to obtain gasdynamic shocks it is necessary to introduce the Riemann's invariants, to split second order equation into two first ones, etc.

The analysis of the front structure can be performed similar to the studies of gas dynamic shocks [22]. In the frame moving with the front, the fluxes are conserved to the right (+) and to the left (-) of the shock, so the front velocity reads [36]

$$V = \frac{\Gamma_n\Big|^{+} - \Gamma_n\Big|^{-}}{n^{+} - n^{-}}. \tag{7}$$

As can be seen from Fig.8 magnitude of V lies in between u^{+} and u^{-}, and if $n^{-} = 0$, $V = u^{+}$ the ion discontinuity moves with a convective velocity, corresponding to the largest density.

Substituting the expression for the negative ion flux Γ_n (6b), into Eq. (7) we have

$$V = \frac{\mu_p \mu_n T_e \dfrac{dn_e}{dx}\Big|^{+}}{\left(\mu_p (n + n_e) + \mu_n n\right)\Big|^{-}} = \frac{\mu_p \mu_n T_e \dfrac{dn_e}{dx}\Big|^{-}}{\left(\mu_p (n + n_e) + \mu_n n\right)\Big|^{+}}. \tag{8}$$

In Ref. 36 good agreement was shown between the theoretical predictions for the front speed Eq.(8) and numerically obtained values. The front structure is quasi stationary; ion diffusion is balanced by convective flux in the frame moving with the front. After straightforward algebra, the front width is [36],

$$L_{front} = 2.2 L_e \frac{T_i}{T_e}\left(3 + \frac{n_e}{n^{+}} + \frac{n^{+}}{n_e}\right), \tag{9}$$

for the case of equal ion mobilities, and $n^{-} = 0$. The front width increases proportionally to ratio of ion to electron temperature, which is typically small ~0.01 in gas discharges. For small electronegativity $n_e >> n^{+}$ $L_{front} \approx 2.2 L_e \dfrac{T_i}{T_e}\dfrac{n_e}{n^{+}}$ front sheath is reciprocal of the change in density in the front (n_{+}); small density discontinuities spreads wider similarly to the shocks in Burgers' equation, where $u_{eff} \sim n$ [22]. In the opposite case $n_e << n^{+}$, $L_{front} \approx 2.2\, L_e \dfrac{T_i}{T_e}\dfrac{n^{+}}{n_e}$ the sheath

width is proportional to the change in density in the front in contrast to the Burgers' equation, and in the range $1/2 < n^+/n_e < 1$ the front width varies insignificantly and $L_{front} \approx 13 L_e \frac{T_i}{T_e}$. If the front width is smaller than ion mean free path, it is determined by ion inertia effects and has an oscillating structure [25].

We have studied many different cases for few EN gases [8, 21, 32, 36]. The negative ion fronts are clearly seen during the active (power "on") glow if: 1) the plasma electronegativity is not very small, $n/n_e > 1/2$, so that the nonlinearity of the negative ion velocity Eq.(6) is important, and 2) an edge region of electron-ion plasma exists, which corresponds to not very high electronegativity at the edge, $n/n_e < \sqrt{T_e/T_i}$.

V. Negative ion fronts in stationary profiles

Figs.1-4 depict regions with sharp variation of negative ion density; fronts are typical for stationary discharges. The question arises: what is the nature of these fronts. Fronts, discussed in previous section, cannot be stationary, since $\Gamma_n(n)$ is a monotonic function and the front velocity Eq.(7) is always positive, V>0. The situation may change when ion mobilities are not constant and decrease with ion density, for example due to momentum exchange in collisions between positive ions and negative ions.

From the other hand, the signal propagation velocity tends to zero rapidly for large electronegativity $u_{eff} \to \frac{\mu_n \mu_p \Gamma_e n_e}{(\mu_n n + \mu_p p)^2}$, so the negative ion flow slows down abruptly at large n/n_e and negative ion pumps up. Indeed, the negative ions are produced at the discharge periphery

due to electron attachment to gas molecules, and drift towards plasma center. The negative ion density is governed by Eq. (4a), which in a stationary case reads:

$$-u_{eff}\frac{\partial n}{\partial x}=\nu_{att}n_e-\gamma_d n-\beta_{ii}np, \qquad (10)$$

and if $u_{eff}\to 0$ $\frac{\partial n}{\partial x}\to\infty$. Thus, fronts appear as an asymptotic limit $n/n_e>>1$ in stationary profiles. The concept of ion discontinuities allows efficient prediction of stationary profiles [17, 20, 37]. The front width is of the order of $L_{front}=\frac{u_{eff}n}{\nu_{att}n_e}$, ion diffusion may spread the front wider, up to a width $L_{front}=\sqrt{\frac{\mu_i T_i}{\gamma_d+\beta_{ii}n}}$. Note, that in contrast to gasdynamic shocks, the width of the stationary front is larger than the nonstationary front width Eq.(9), and is determined by the negative ion source. This is due to the fact that effective mechanism of front compression due to overturning is absent for stationary profiles.

VI. Negative ion fronts in afterglow

In the afterglow the power is switched off, and the plasma decays due to wall and volume losses, the electron temperature drops simultaneously. A new kind of negative ion front appears in the discharge afterglow if electron temperature remains high enough, $T_e>>T_i$. The electron temperature can be elevated in the afterglow due to two reasons: 1) metastables heat electrons in superelastic collisions, and 2) there can be a small residual power in the afterglow; in practical situations this may correspond to capacitively coupled biasing of an otherwise inductively coupled pulsed discharge, see for example Ref. 40. Solving the heat conduction equation (3) we found that a

residual power as small as 0.1% of the power during the active glow can keep electrons warm with T_e~*1* eV, see more details in Ref. 21, 32. In Fig. 6 the spatial profiles of densities and fluxes for both electrons (dashed lines) and negative ions (solid lines) are shown in the afterglow (50-200 μs after power is switched off), when the electron density is much smaller than the initial value of 4.2 10^8 cm^{-3}, the electron temperature was fixed at a value 1 eV in the afterglow. The electron density keeps decreasing mainly due to wall losses, while the total negative ion density remains nearly constant. Negative ions are trapped in the discharge by the large electric field at the periphery region. Wall losses of negative ions are negligible when electrons with $T_e >> T_i$ are still present.

The frequency of electron loss $Z_{e,loss}$, which is determined by the slow diffusion in the edge region, is nearly constant as can be deduced from the exponential decay of electron density in Fig. 6. The electronegativity ratio n/n_e is very large at the discharge center (ion-ion core) and approaches zero near the edge. Therefore, D_{eff} (Eq. 4b) is very inhomogeneous, large in the ion-ion core region $\approx \mu_i T_e n / n_e$ and small in the edge region $\approx \mu_i T_e$. At the edge region of electron-ion plasma ($L_{ii}<x<L$), the electron density is described by a linear diffusion equation: $\frac{\partial n_e}{\partial t} = D_{amb} \frac{\partial^2 n_e}{\partial x^2}$, here L_{ii} is the extent of the ion-ion core and L is half of the interelectrode gap. The boundary condition at $x=L_{ii}(t)$ is $D_{amb} \frac{\partial n_e}{\partial x} = \frac{\partial n_e}{\partial t} L_{ii}(t)$, which is a consequence of continuity at $0<x<L_{ii}$. This equation has an analytic solution: $n_e(x,t) = n_e(0,0) \frac{sin(\kappa(L-x))}{sin(\kappa(L-L_{ii}))} e^{-Z_{e,loss}t}$, where $Z_{e,loss} = D_{amb}\kappa^2$, and $kL_{ii}\, tan(k(L-L_{ii})) = 1$. For example, for $L_{ii}=0.5L$ one obtains $\kappa L = 1.722$, and the electron loss frequency is only *20%* higher than in the case of a uniform diffusion coefficient ($\kappa L = \pi/2$), for $L_{ii}=0.7L$ the electron loss frequency is only 1.7 times higher, and eventually at $L_{ii} \to L$

$Z_{e,loss} \to D_{amb} / L /(L - L_{ii})$. Thus, even though $L_{ii}(t)$ changes with time, $Z_{e,loss}$ varies insignificantly with L_{ii}.

The negative ion motion is governed by the competition of diffusion and drift. In the ion-ion plasma core, $n >> n_e$, and for $\mu_n = \mu_p$ $\Gamma_n \approx -\Gamma_e / 2$, and Eq. (4) simplifies to,

$$\frac{\partial n}{\partial t} = \frac{\partial}{\partial x}(D_i \frac{\partial n}{\partial x}) + \frac{1}{2}(Z_{ioniz} n_e - \frac{\partial n_e}{\partial t}). \quad (11)$$

Note, that Eq. (11) is also valid at the steady-state (with the time derivative terms set equal to zero). In the afterglow $Z_{ioniz} \approx 0$ and $\frac{\partial n_e}{\partial t} = -Z_{e,loss} n_e$. As discussed above $Z_{ioniz,st} = \mu_i T_{e,st} \kappa^2$ and $Z_{e,loss} = \mu_i T_{e,aft} \kappa^2$ where $T_{e,st}$ and $T_{e,aft}$ are electron temperature at the steady state and the afterglow, respectively. Thus, at the very beginning of the afterglow, the first term on the r.h.s of Eq.(11) is equal to the second term, and the negative ion density remains the same. When T_e has quickly dropped to a fraction of its original value due to inelastic processes, the second term on the r.h.s. of Eq.(11) is small and the first term dominates. This implies that negative ions diffuse almost freely in this region and thus drift is small compared to diffusion. In the ion-ion plasma core ($n_e << n$) the positive and negative ion fluxes coincide (see Fig.6). As the negative ion density decreases towards the edge, the electric field increases, reducing the negative ion flux to practically zero. Thus, free ion diffusion is slowed down, since the electric field retards the motion of negative ions. The electric field can be found from Eq. (4b). The electron density is uniform in the ion-ion plasma core, and $\Gamma_e = x \frac{\partial n_e}{\partial t} = x Z_{e,loss} n_e$. The electron flux increases towards the wall, where the negative ion density drops, so the electric field $E = \frac{T_e}{n_e} \frac{\partial n_e}{\partial x} \approx \frac{\Gamma_e}{b_i (p + n)} = \frac{x Z_{e,loss} n_e}{b_i (n_e + 2n)}$ increases towards the edge where n_e / n is large. As the electric field magnifies, the drift flux of negative ions

equalizes the diffusive flux and, at some point, the net negative ion flux is reduced to $\Gamma_n << \Gamma_e$. At that point, negative ions are almost in Boltzmann equilibrium, $T_i \frac{\partial n}{\partial x} \approx T_e \frac{n}{n_e} \frac{\partial n_e}{\partial x}$. This implies that the negative ion density drops nearly exponentially, $n \sim exp(-x/\delta)$, where $\delta = \frac{T_i}{T_e}\left(\frac{\partial\, ln(n_e)}{\partial x}\right)^{-1}$, towards the edge plasma forming a negative ion front. The front can be seen clearly in Fig. 6.

The transition from nearly free negative ion diffusion (ion-ion core) to negative ion Boltzmann equilibrium occurs at the point where the diffusion flux becomes of the order of the drift flux (say three times larger). Therefore, the point where the negative ion density starts dropping rapidly can be estimated from the condition of equality of electron and ion fluxes $\Gamma_n = \Gamma_e = \Gamma_p / 2$. At this point, the negative ion diffusion flux is three times larger than their drift flux. Substituting expressions for fluxes $\Gamma_n = \mu_i T_i \frac{\partial n}{\partial x}$ and $\Gamma_e = x\, Z_{e,loss} n_e$, we find the equation for front propagation,

$$\mu_i T_i \left.\frac{\partial n}{\partial x}\right|_{x_{if}} = Z_{e,loss} n_e x\Big|_{x_{if}} . \tag{12}$$

The negative ion density profile in the ion-ion core can be from Eq.(11) neglecting second term in r.h.s. Assuming that negative ions diffuse a large distance compared to the initial extent of the ion-ion plasma core L_{ii0}, the solution of Eq.(11) for time $t > t_{ii} \equiv L_{ii0}^2 / D_i$, is

$$n(x,t) = \frac{\int n(x,0)dx}{\sqrt{4\pi D_i \tau}} e^{-\frac{x^2}{4D_i\tau}}, \tag{13}$$

where $\tau = t - t_{ii}$. Substituting *n(x,t)* into Eq. (12) and $n_e(\tau) = n_e(t_{ii})\, exp(-Z_{e,loss}\tau)$ we find,

$$-\frac{x_{if}^2}{4D_i\tau} = -Z_{e,loss}\tau + ln(B), \tag{14}$$

where $B = Z_{e,loss} n_e(t_{ii}) 4\tau\sqrt{\pi D_i \tau} / \int n dx$. Free ion diffusion starts at time t_{ii}, when $D_i \frac{\partial^2 n}{\partial x^2} \sim 0.5 Z_{e,loss} n_e$, so that B~1. Accordingly, for long times, $Z_{e,loss}\tau > 1$, Eq.(14) yields,

$$x_{if} = V_{if}\tau, \text{ with } V_{if} = 2\sqrt{D_i Z_{e,loss}} \quad (15)$$

Surprisingly, the negative ion front moves with nearly constant velocity V_{if}. Note, that Eq. (15) is not exact as is Eq.(7) for an active glow, but valid only approximately, when Eq.(14) and $Z_{e,loss} \approx const$. holds.

In Fig. 6 the points corresponding to $\Gamma_n = \Gamma_e$ (top) and $n_e = n$ (bottom) are shown. From this figure, one finds the velocity of the point at which $\Gamma_n = \Gamma_e$ as 2.6 10^4 cm/s, close to the analytic estimate (Eq. 14) of V_{if} = 3.2 10^4 cm/s. The velocity of the point at which $n_e = n$ is 1.6 10^4 cm/s, close to $V_{if} / 2$. The velocity of the point at which $n_e = n$ is lower, since in this region $\Gamma_n < \Gamma_p$ (see Fig.6), and the electric field retards ion free diffusion. We checked the velocity of propagation of the point at which $n_e = n$ for different discharge conditions. Interestingly, for all conditions, this velocity was close to $V_{if} / 2$ [32]. In classical gasdynamics, the shock velocity lies between these two velocities. We note that, in contrast to this, the velocity of the negative ion front in the afterglow is larger than the velocity of the negative ions everywhere in the discharge.

VII Conclusions

In this paper, we have demonstrated that weakly damped perturbations propagate in collisional multi-species weakly ionized plasmas with a speed $u_{eff} = \frac{\mu_p n_e}{\mu_n n + \mu_p p} u$, where u is the

negative ion drift velocity. Due to the nonlinear dependence of the signal speed on the ion density, discontinuities in ion density (ion fronts) may appear due to steepening of ion density profiles, analogous to gasdynamic shocks. Note, that these fronts are different from collisionless shocks and shocks in fully ionized plasma. The width of the front is proportional to the ratio of the ion to the electron temperature multiplied on the electron inhomogeneity scale.

The ion fronts have been also observed in stationary discharges. These fronts are not the result of profile breaking and appear as an asymptotic limit $n/n_e >> 1$ in which ion signal propagation speed tends to zero. In contrast to nonstationary fronts, width of the stationary front is larger and is determined by the negative ion production source. This is owing to the fact that effective mechanism of front compression due to steepening is absent for stationary profiles.

When $T_i << T_e$, other kind of negative ion density fronts may form during the afterglow also. These fronts are not analogous to gasdynamic shocks. Negative ions diffuse freely in the plasma core, but the negative ion front propagates towards the chamber walls with a nearly constant velocity $V_{if} = \sqrt{4 D_i Z_{e,loss}}$ in contrast to diffusive front velocity $\sim \sqrt{D_i / t}$. The negative ion fronts are a new type of nonlinear structure, different from gasdynamic nonlinear waves and beyond the classification of dissipative structures (see for example Ref. 11).

Acknowledgment

Author thanks Profs. R.N. Franlkin and L.D. Tsendin for persistent encouragement to complete the study of negative ion nonlinear phenomena. Discussions with E. Startsev and G. Shvets are greatly acknowledged. The work of was funded by the National Science Foundation, CTS-9713262, and by Alexander von Humboldt Foundation.

References

[1] M.A. Lieberman and A.J. Lichtenberg, *Principles of Plasma Discharges and Materials Processing* (Wiley, NY 1994).

[2] G S Hwang and KP Giapis, , Phys. Rev. Lett. **79**, 845 (1997).

[3] M Hopkins and K Mellon, Phys. Rev. Lett. **67**, 449 (1991).

[4] W Swider, Ionospheric Modeling (Birkhauser Verlag, Basel, 1988).

[5] V.N. Tsytovich, Comments on Plasma Physics & Controlled Fusion, **1** part C, 41 (1999).

[6] Y. Watanabe, M. Shiratan, Y. Kubo, I.Ogawa and S. Ogi, Appl. Phys. Lett. **53**, 1263 (1988)

[7] C. Charles, R. Boswell, and H. Kuwara, Appl. Phys. Lett. **67**, 40 (1995)

[8] V. Midha and D. Economou, "Spatio-temporal evolution of a pulsed chlorine discharge", submitted to Plasma Sources Sci. Tecnol.

[9] B. A. Smith and L. J. Overzet, Plasma Sources Sci. Technol. **8**, 82 (1999).

[10] M.V. Malyshev, V.M. Donnelly, Samukawa, S., J. Appl. Physics, **86,** 4813 (1999).

[11] B.S. Kerner, V.V. Osipov, Soviet Physics, Uspekhi, **33**, 679 (1990).

[12] J. B. Thompson, Research Notes, Proc. Royal Soc. **73**, 818 (1959); G. L. Rogoff, J. Phys. D: Appl. Phys., **18**, 1533 (1985). A. J. Lichtenberg, V. Vahedi, M. A. Lieberman, T. Rognlien, J. Appl. Phys. **75**, 2339 (1994).

[13] M. V. Konjukov, Sov. Phys. JETP, **34**, 908; 1634 (1958). (in Russian). , H. Sabadil, Beitr. Plasmaphys., **13**: 235 (1973). G. A. Galechjan, in Plasma Chemistry, Editor: B. M. Smirnov, v.7 (Moscow: Atomizdat) 1980, 218-251. (in Russian).

[14] R.N. Franklin and J.Snell, J. Phys. D: Appl. Phys. **32**, 2190 (1999); J. Plasma Phys. **64**, 131 (2000)

[15] Rozhansky V.A, Tsendin L.D., *Transport Phenomena in Partially Ionized Plasmas* (Energoizdat, Moscow 1988 in russian), (Gordon & Breach, NY, 2000).

[16] A.P.Dmitriev, V.A. Rozhansky, L.D.Tsendin. Sov.Phys. - Uspekhi, **28**, 467 (1985).

[17] L. D. Tsendin, Sov. Phys. Tech. Phys., **34**, 11 (1989)

[18] P.G. Daniels and R.N. Franklin, J. Phys. D: Appl. Phys. **22**, 780 (1989); P.G. Daniels, R.N. Franklin and J.Snell, ibid **23**, 823 (1990); R.N. Franklin, P.G. Daniels and J.Snell, ibid **26**, 1638 (1993); R.N. Franklin and J.Snell, ibid **27**, 21823 (1990).

[19] V. N. Volynets, A.V. Lukyanova, A. V. Rakhimov, et al. , J. Phys. D: Appl. Phys. **26**, 647 (1993).

[20] I. D. Kaganovich, L. D. Tsendin, Plasma Phys. Reports, **19**, 645 (1993).

[21] I. Kaganovich, B. N. Ramamurthi, and D.J. Economou, Phys. Rev. Lett. **84**, 1918 (2000)

[22] G. B. Whitham, *Linear and Nonlinear Waves* (Wiley, NY, 1974).

[23] T. Takeuchi, S. Iizuka,and N. Sato, Phys. Rev. Lett. **80**, 77 (1998).

[24] V Kolobov and D Economou, Appl. Phys. Lett. **72**, 656 (1998).

[25]I. G. Kouznetsov, A.J. Lichtenberg, M. A. Lieberman; J. Appl. Phys. **86,** 4142 (1999)

[26] F. Kolrausch, Ann. Phys. Chem. **62**, 209 (1897).

[27] H. Weber, Sitz. Akad. Wiss. Berlin **44**, 936 (1897).

[28] Aleksandrov N.L.,Napartovich A.P.Sov. Phys.- Uspekhi, **163**, 1 (1993) (in Russian).

[29] F. I. Visikailo, Sov. J. Plasma Phys., **11** 1256 (1985) (in Russian).

[30] D. Vender, W.W. Stoffels, E. Stoffels, G.M.W. Kroesen, and F.J. de Hoog, Phys. Rev. E **51**, 2436 (1995).

[31] U. Buddemeier Ph.D. Thesis Ruhr Universitaet 1997, S.V. Berezhnoi, U. Buddemeier, I. Kaganovich, C.B. Shin, Appl. Phys. Lett., **77**, 800 (2000)

[32] I.D. Kaganovich, B. N. Ramamurthi and D.J. Economou, Appl. Phys. Lett., **76**, 284 (2000); and submitted in Phys. Rev.E

[33] S. Ashida and M.A. Lieberman, Jpn. J. Appl. Phys., **36**, 854 (1997).

[34] R.R. Arslanbekov, A. A. Kudryvtsev, Phys. Rev. E, **58**, 7785 (1998).

[35] Z. Wang, A.J. Lichtenberg, and R.H. Cohen, Plasma Sources Sci. Technol. **8**, 151 (1999)

[36] I. Kaganovich , S.V. Berezhnoi , C.B. Shin, "Signal Propagation in Collisional Plasma with Negative Ions", submitted to Phys. Of Plasmas

[37] A.J. Lichtenberg, I. Kouznetsov, Y.T. Lee, M.A. Lieberman, I.D. Kaganovich, L.D. Tsendin, Plasma Sources Sci. Technol., **6**, 437 (1997).

[38] V. A. Schweigert, *Plasma Phys. Repts.* **17** 844 (1991). (in Russian).

[39] J.P.P. Passchier, W. J. Goedheer, *J. Appl. Phys.* **73**, 1073 (1993).

[40] L.J. Overzet, Yun Lin, and L. Luo, J.Appl.Phys. 72, 5579, (1992).

Figure captions

Fig.1 Symmetrical capacitively coupled discharge RF discharge, oxygen pressure 0.21Torr, from [31]

Fig.2 The experimental negative ion density profiles in the *RF* discharge in oxygen, pressure 100mtorr, frequency 13.56MHz, input power 10W [30].

Fig. 3 The profiles of the charged particle densities obtained in the simulations [38] for SF_6. The trace 1 corresponds to the positive ion density, and 2 - to the time-averaged electron density. The discharge parameters are pressure 0.13 Torr, frequency - 13.6MHz, current density 2mA/cm^2.

Fig. 4 The profiles of the charged particle densities obtained in the simulations [39] for rf discharge in CF_4 gas. The discharge parameters are pressure 0.5 Torr, frequency - 13.6MHz.

Fig.5 Negative ion (solid lines) and electron density - (dashed lines) in the early discharge active glow. Interelectrode gap 10 cm, mixture of 97% Ar and 3% O_2 of total pressure 5mTorr, averaged power density 1.0 mW/cm^2 , pulse duration 600 μs, duty ratio 0.5.

Fig.6 Spatial profiles of fluxes and densities of negative ions (solid lines) and electrons (dashed lines) in afterglow for the conditions of Fig.5. The points where $\Gamma_n = \Gamma_e$ and n_e=n are shown as circles.

Fig. 7 Propagation of small signal for the same unperturbed electron density (n_e =*3.7-0.3 x*) and different densities of unperturbed plasma negative ions. (a) $n \approx 2.0\, n_e$ (*n =6-0.3 x),* (b) $n \approx n_e$ (*n =4-0.3 x),* (c) $n = 0$. All variables are dimensionless, normalized on some reference values, density n / n_0 ,

coordinate *x/L*, time $tL^2/(\mu_n T_e)$. Ion diffusion was neglected, and ion nobilities were taken to be the same $\mu_n = \mu_p$.

Fig.8 Negative ion flux as function of electronegativity, Arrows denote negative ion convective velocity $u = \frac{\Gamma_n}{n}$, small signal propagation velocity $u_{eff} = \frac{\partial \Gamma_n}{\partial n}$, and ion discontinuity ($n_+ \rightarrow n_-$) propagation velocity $V = \frac{\Gamma_n\big|_+ - \Gamma_n\big|_-}{n_+ - n_-}$.

Fig. 9 Propagation of large perturbation of negative ion density for the conditions of Fig.1, but n_e *=6.2-3.6x,* initially at *t=0* $n = \frac{N}{a\sqrt{\pi}} \exp\left(-\frac{(x-0.93)^2}{a^2}\right)$, where *a=0.0144,* and total number of negative ions *N=0.476,* and negative ion density profiles are plotted 6 times every 0.25 units of dimensionless time.

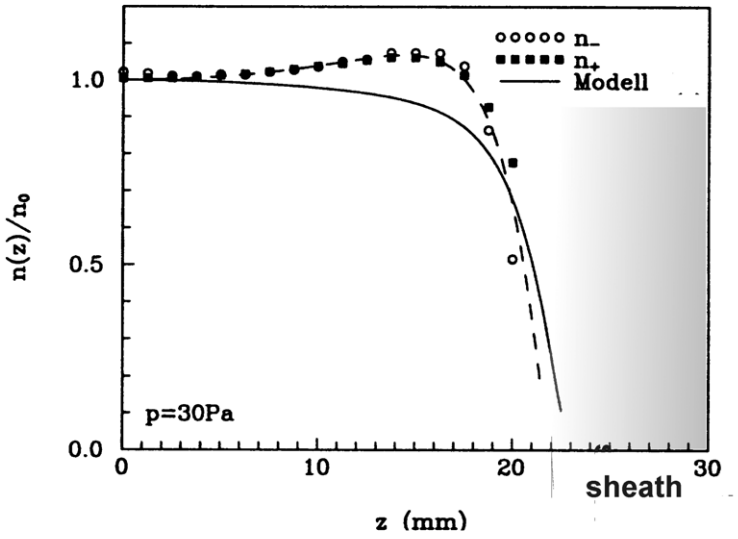

[1] Fig.1 Kaganovich

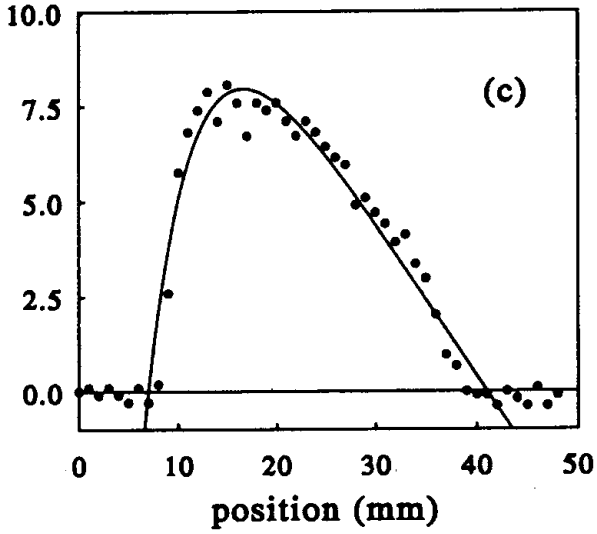

[2] Fig.2 Kaganovich

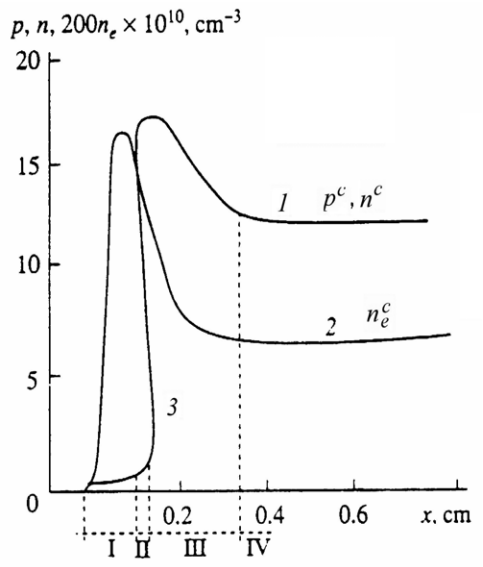

[3] Fig.3 Kaganovich

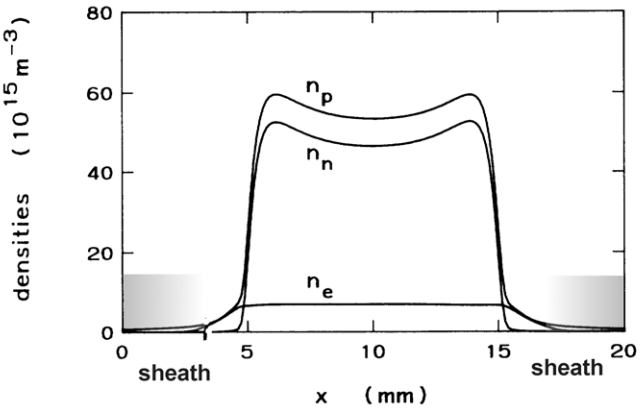

[4] Fig.4 Kaganovich

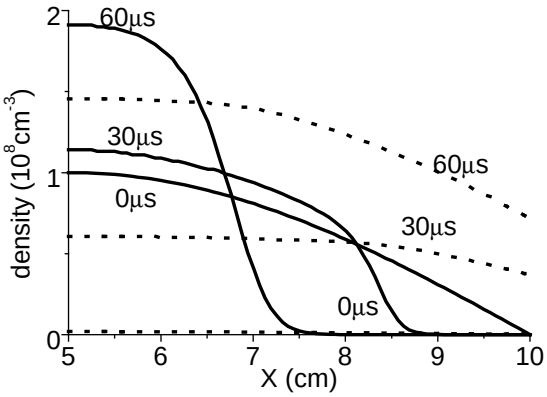

[5] Fig.5 Kaganovich

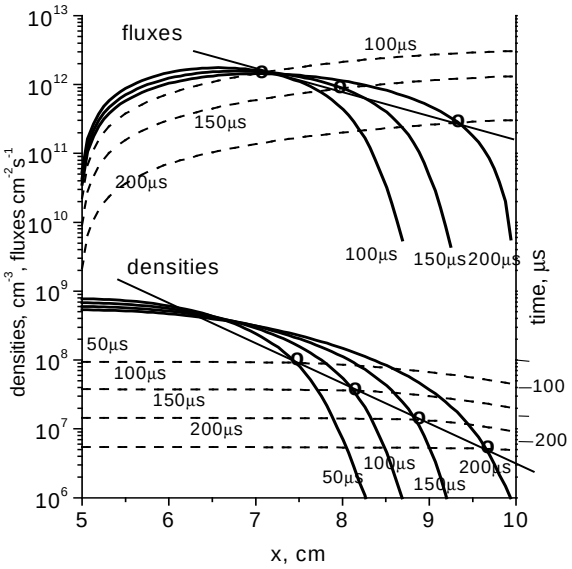

[6] Fig.6 Kaganovich

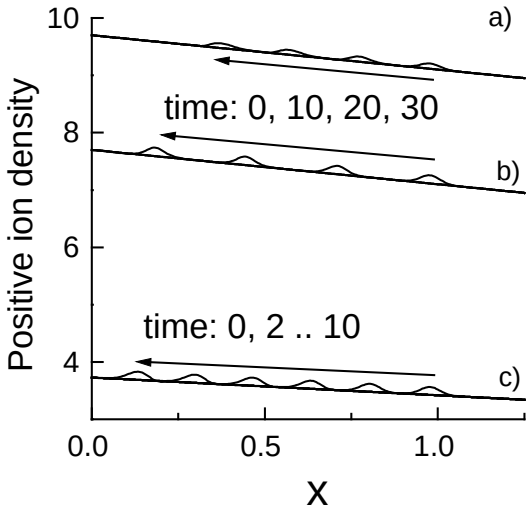

[7] Fig.7 Kaganovich

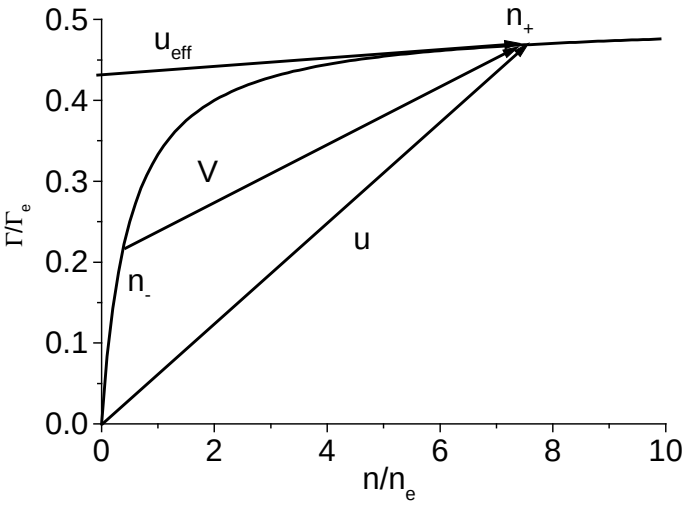

[8] Fig.8 Kaganovich

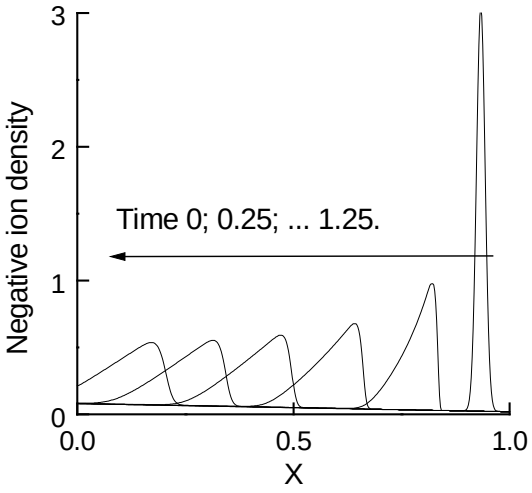

[9] Fig.9 Kaganovich

The Princeton Plasma Physics Laboratory is operated
by Princeton University under contract
with the U.S. Department of Energy.

Information Services
Princeton Plasma Physics Laboratory
P.O. Box 451
Princeton, NJ 08543

Phone: 609-243-2750
Fax: 609-243-2751
e-mail: pppl_info@pppl.gov
Internet Address: http://www.pppl.gov